Supporting Materials for

Silicon(IV) complexes of octaaryl substituted porphyrazines and corrolazines: Influence of the macrocycle contraction on spectral-luminescence, acid-base and redox properties

Ekaterina D. Rychikhina, Svetlana S. Ivanova, Veronika Novakova, Pavel A. Stuzhin

[a] *Research Institute of Macroheterocycles, Ivanovo State University of Chemistry and Technology, RF-153000 Ivanovo, Russia.*
[b] *Faculty of Pharmacy in Hradec Kralove, Charles University, 500 05 Hradec Kralove, Czech Republic*

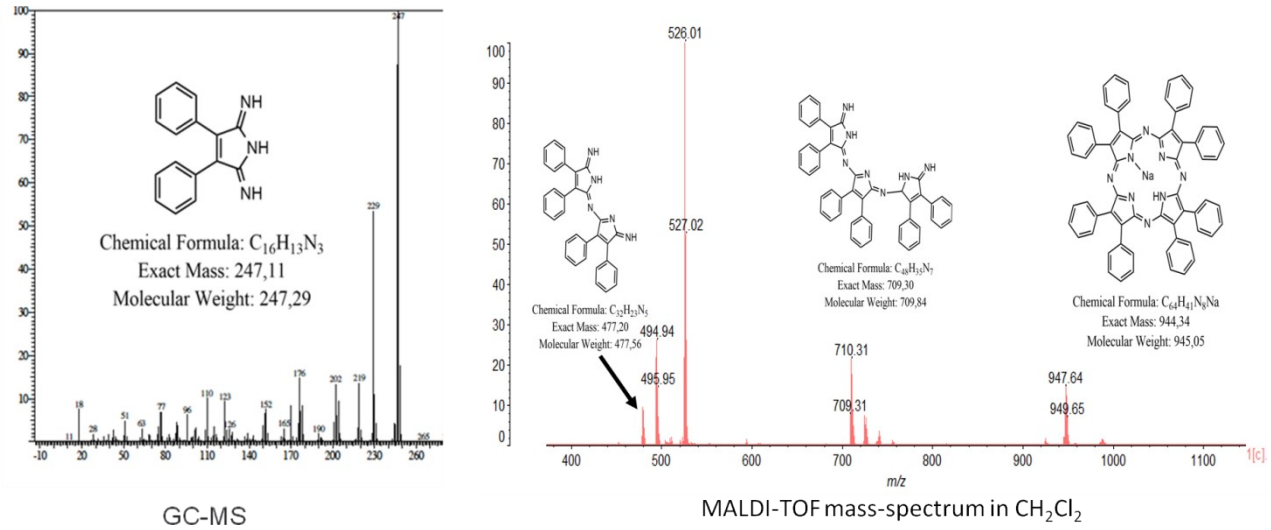

Figure S1. Chromato mass spectrum and MALDI TOF mass spectrum of the reaction mixture of diminoimide synthesis, illustrating the formation of its oligomerization.

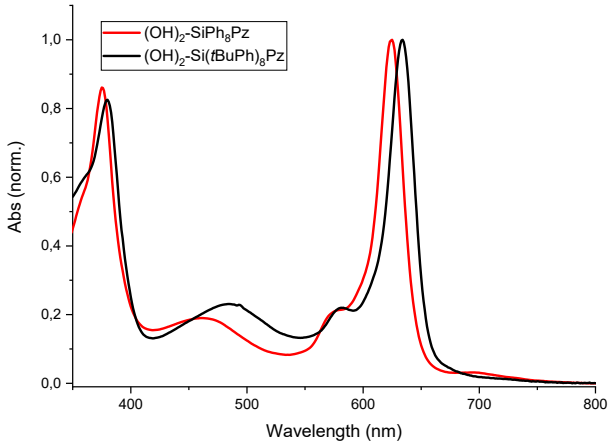

Figure S2. UV-vis spectra of the dihydroxy silicon octaarylporphyrazines in CH_2Cl_2.

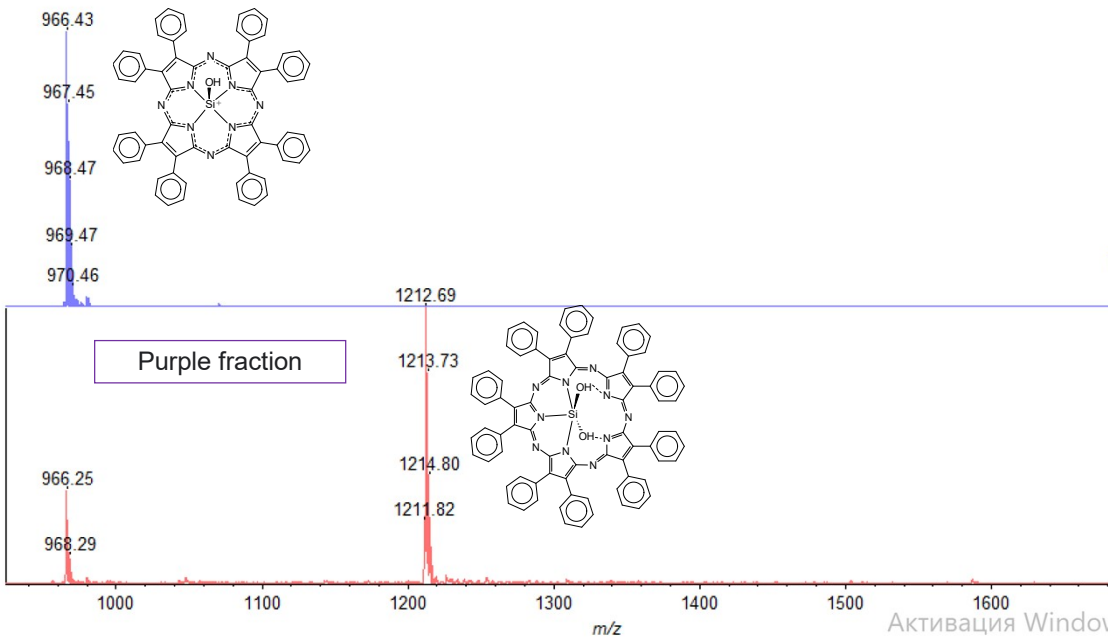

Figure S3. The mass spectra of compound **3a** (Si octaphenylporphyrazine) and presumably its pentapyrrolic derivative, contained in the purple fraction.

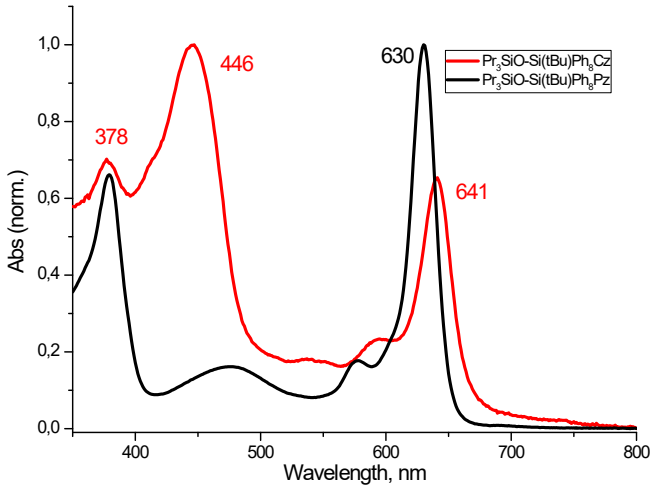

Figure S4. The absorption spectra of $(Pr_3SiO)SiCz(^tBuPh)_8$ **(5b)** and its porphyrazine precursor $(Pr_3SiO)_2SiPz(^tBuPh)_8$ (**4b**) in CH_2Cl_2.

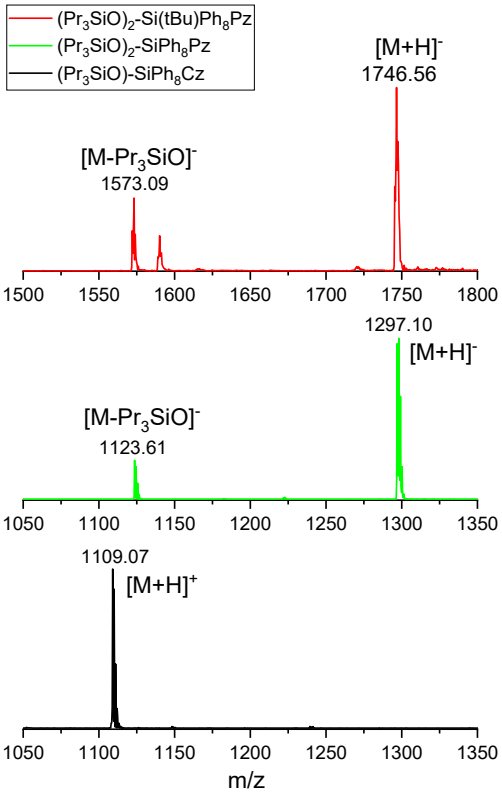

Figure S5. MALDI-TOF mass spectra of $(Pr_3SiO)_2SiPzPh_8$ (**4a**) (green line), $(Pr_3SiO)_2SiPz(^tBuPh)_8$ (**4b**) (red line) and $(Pr_3SiO)SiCzPh_8$ (**5a**) (black line).

IR spectra of the SiPz and SiCz complexes

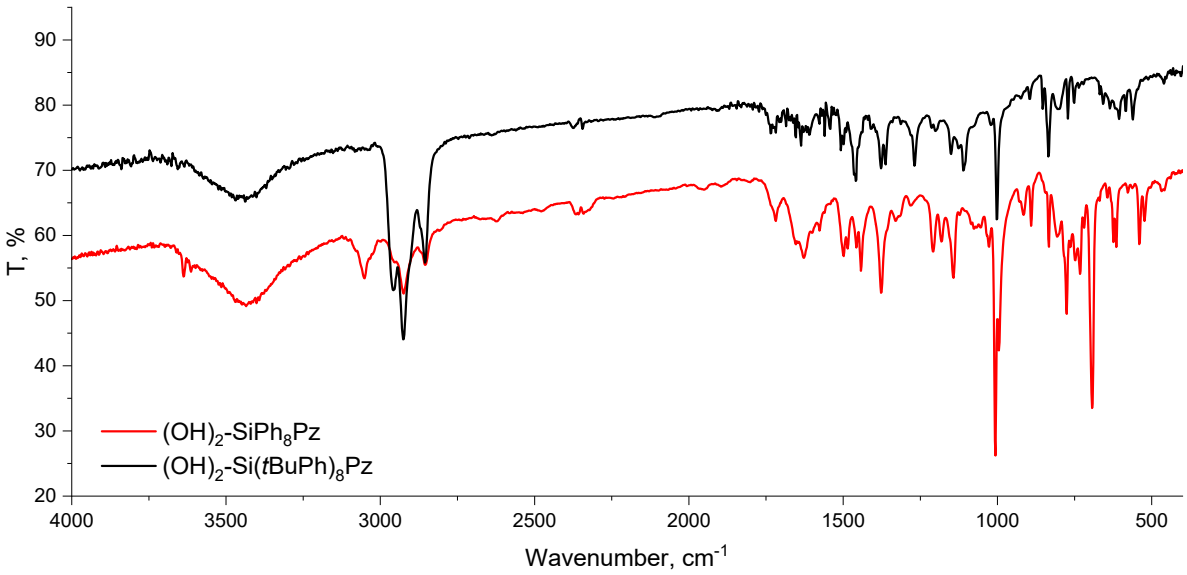

Figure S6,A. The IR spectra of the dihydroxy silicon octaarylporphyrazines **3a,b**.

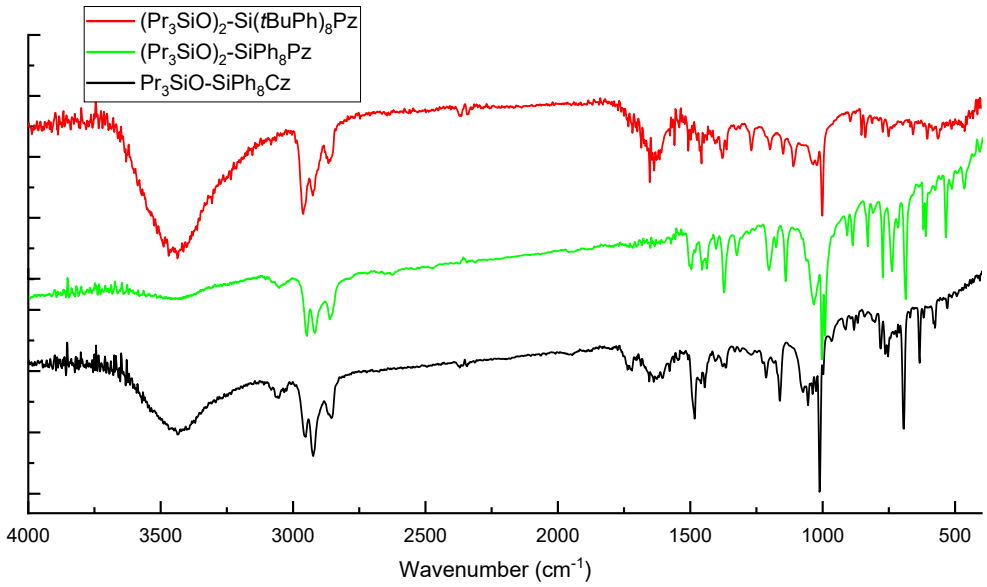

Figure S6,B. IR spectra of $(Pr_3SiO)_2SiPzPh_8$ (**4a**) (green line), $(Pr_3SiO)_2SiPz(^tBuPh)_8$ (**4b**) (red line) and $(Pr_3SiO)SiCzPh_8$ (**5a**) (black line) (KBr pellet)

NMR spectra of the SiPz and SiCz complexes

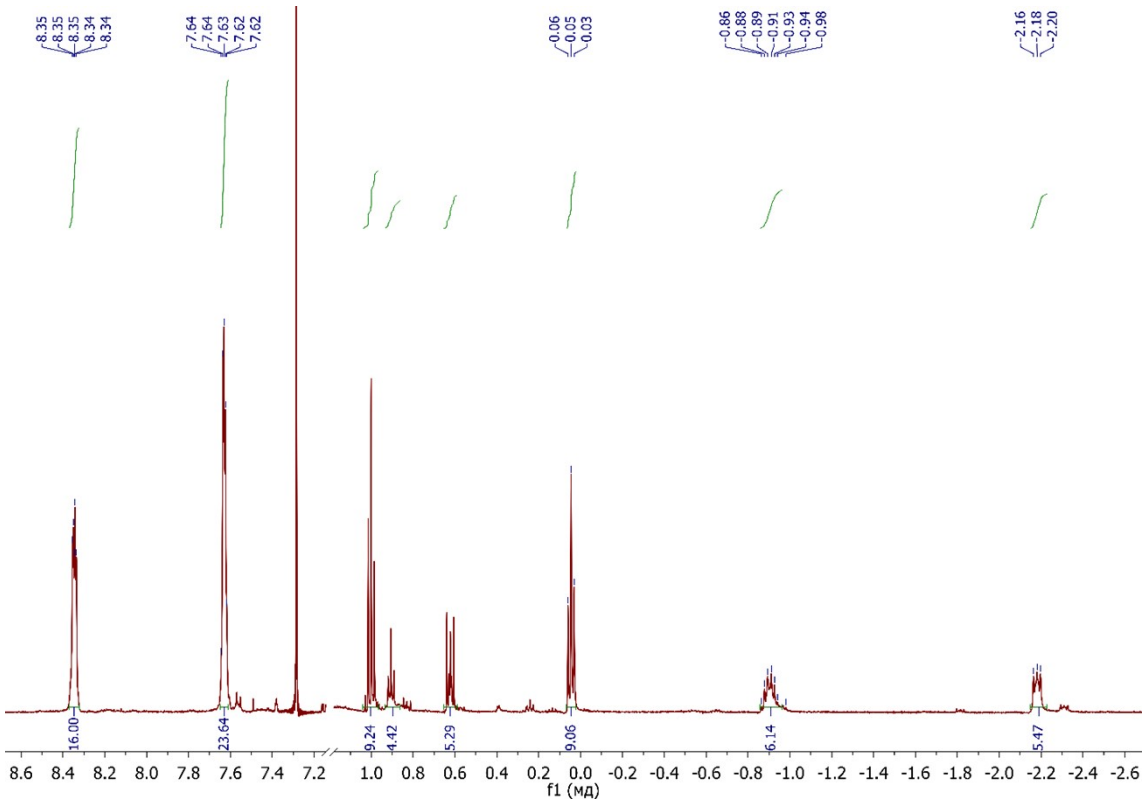

Figure S7,A. ^{1}H NMR spectrum of $(Pr_3SiO)_2SiPzPh_8$ **(4a)** in $CDCl_3$.

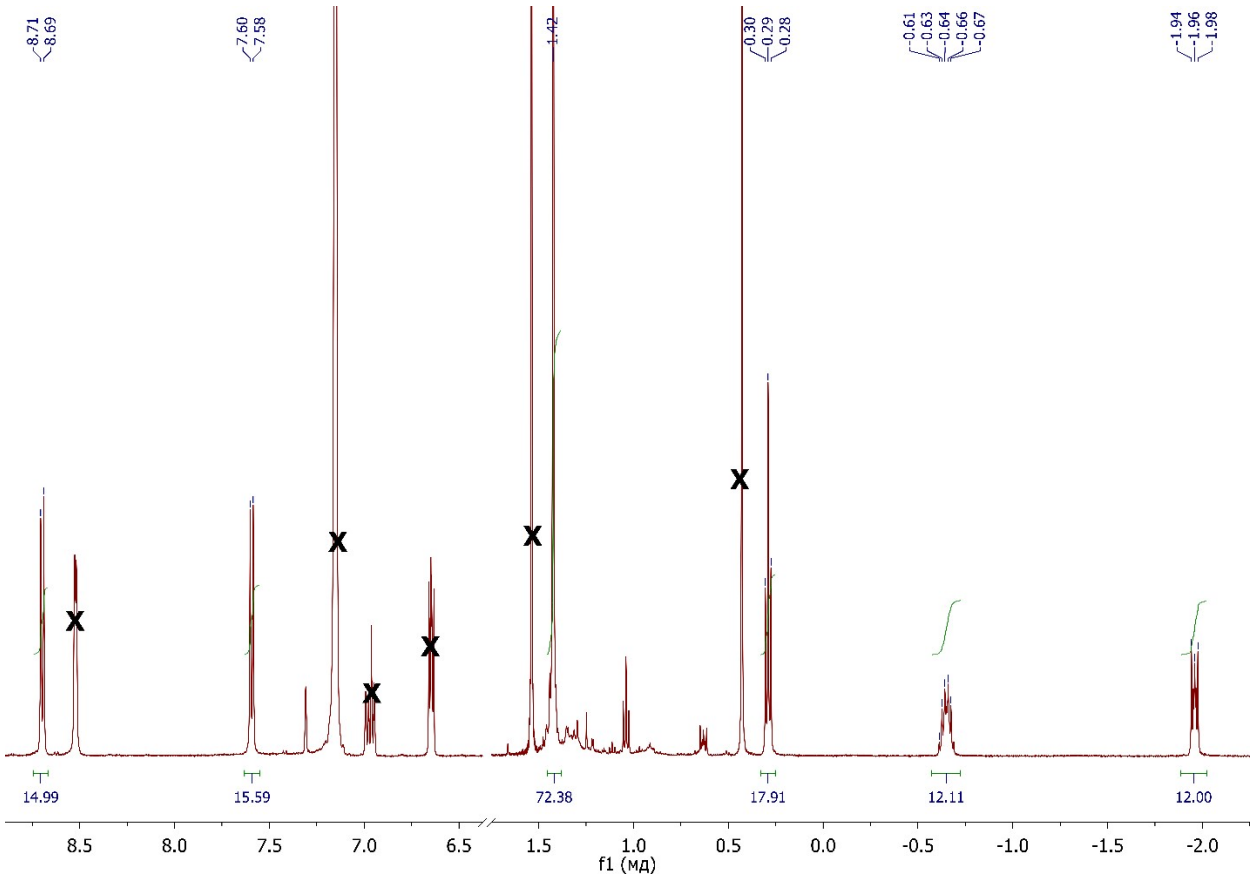

Figure S7,B. ^{1}H NMR spectrum of $(Pr_3SiO)_2SiPz(^{t}BuPh)_8$ (**4b**) in C_6D_6.

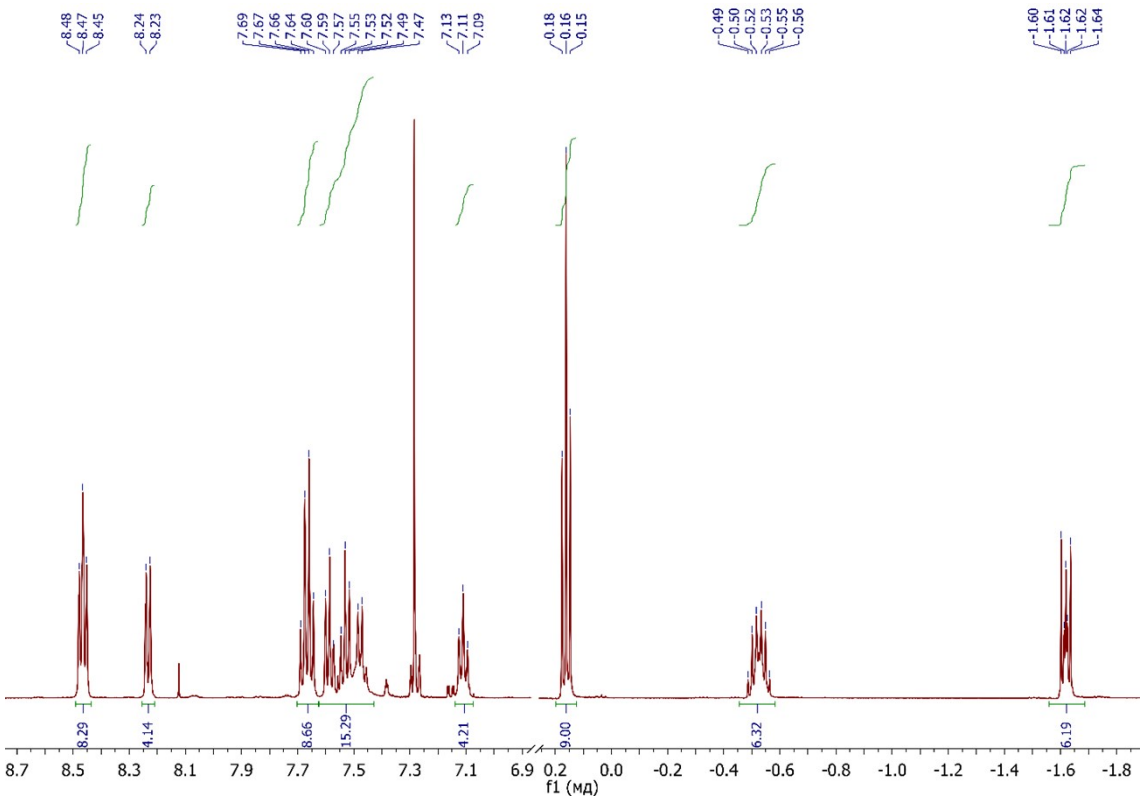

Figure S7,C. ^{1}H NMR spectrum of $(Pr_3SiO)SiCzPh_8$ (**5a**) in $CDCl_3$.

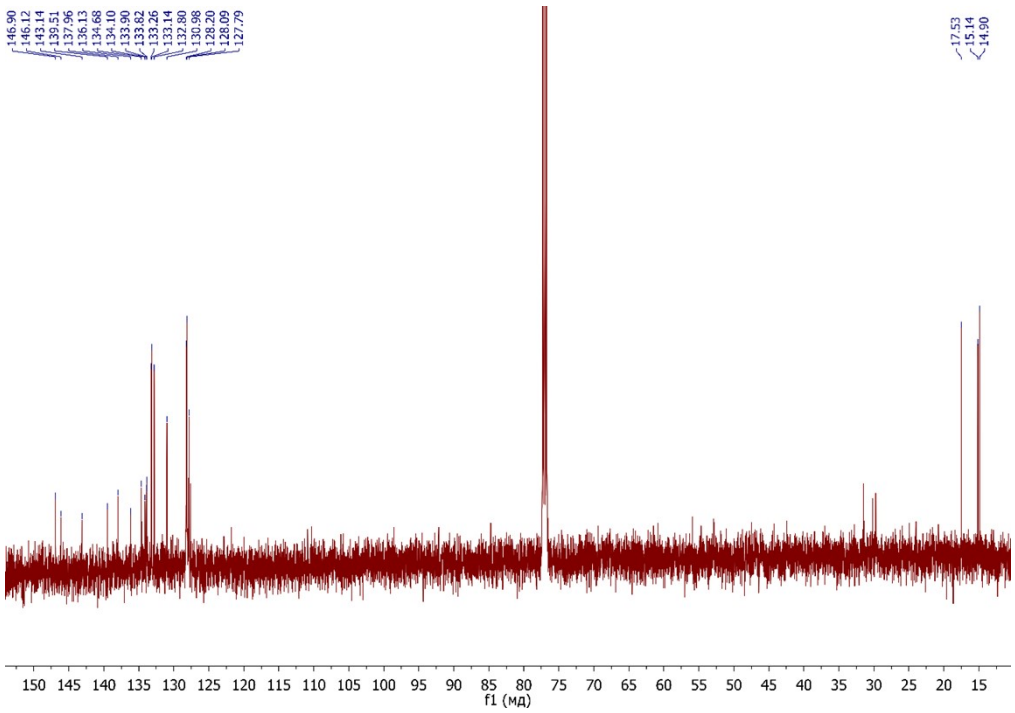

Figure S7,D. ^{13}C NMR spectrum of $(Pr_3SiO)SiCzPh_8$ (**6a**) in $CDCl_3$.

Photopysical properties of the SiPz and SiCz complexes

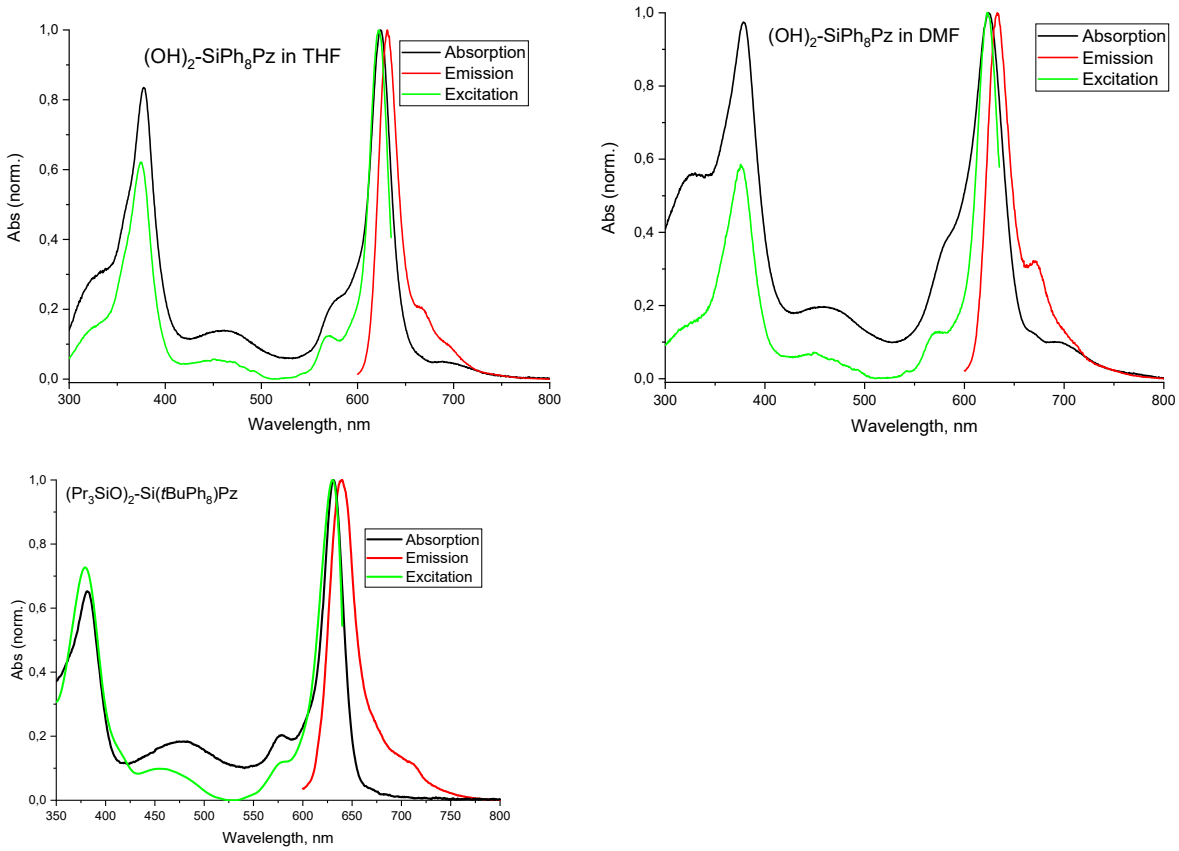

Figure S8,A. Absorption (black line), emission (red line) and excitation (green line) of $(HO)_2SiPzPh_8$ **(3a)** in THF and DMF, and $(Pr_3SiO)_2SiPz(^tBuPh)_8$ (**4b**) in DMF (λ_{ex} = 590 nm, λ_{em} = 660 nm).

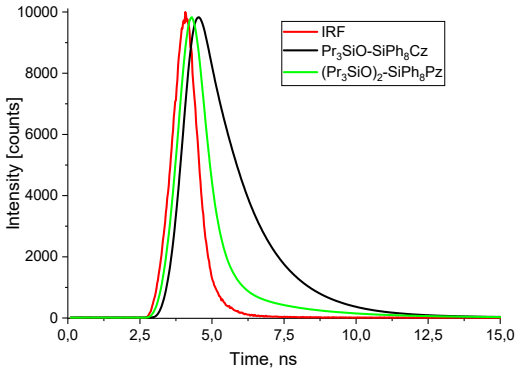

Figure S8,B. Fluorescence decay for $(Pr_3SiO)_2SiPzPh_8$ **(4a)** and $(Pr_3SiO)SiCzPh_8$ **(5a)** in DMF. Excitation wavelength λ_{ex} = 600 nm.

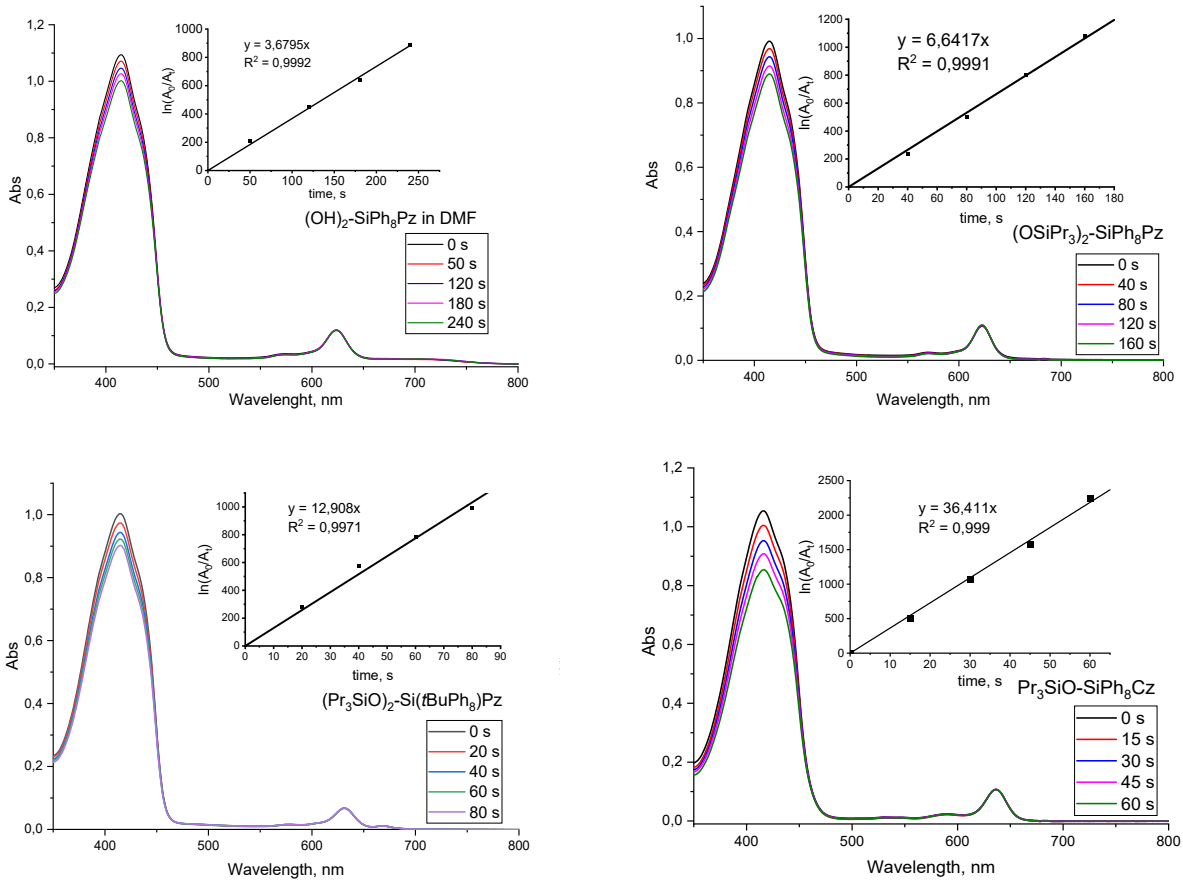

Figure S9. The changes of absorption spectra upon irradiation time in air saturated DMF solution containing DPBF and the photosensitizer (Si complex). Insets: logarithmic dependencies of absorbance on irradiation time at 415 nm.

Electrochemical properties of the SiPz and SiCz complexes

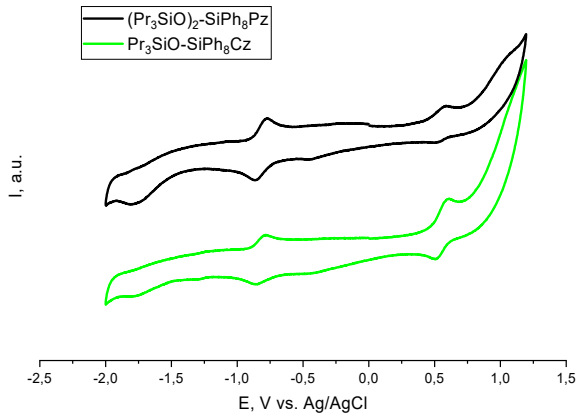

Figure S10,A. Cyclic voltamograms of $(Pr_3SiO)_2SiPzPh_8$ **(4a)** (black line) and $(Pr_3SiO)SiCzPh_8$ **(5a)** (green line) in pyridine with ferrocene. Sweep rate was 25 mV/s.

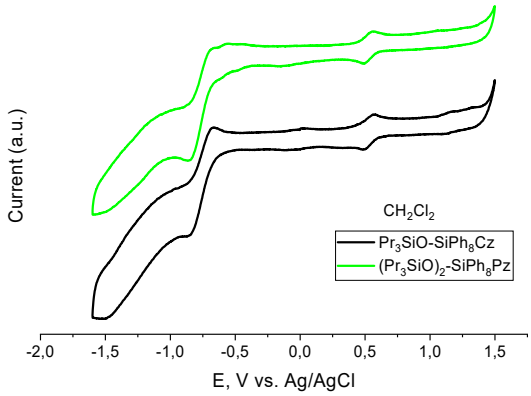

Figure S10,B. Cyclic voltamograms of $(Pr_3SiO)_2SiPzPh_8$ **(4a)** (green line) and $(Pr_3SiO)SiCzPh_8$ **(5a)** (black line) in CH_2Cl_2 with ferrocene. Sweep rate was 25 mV/s.

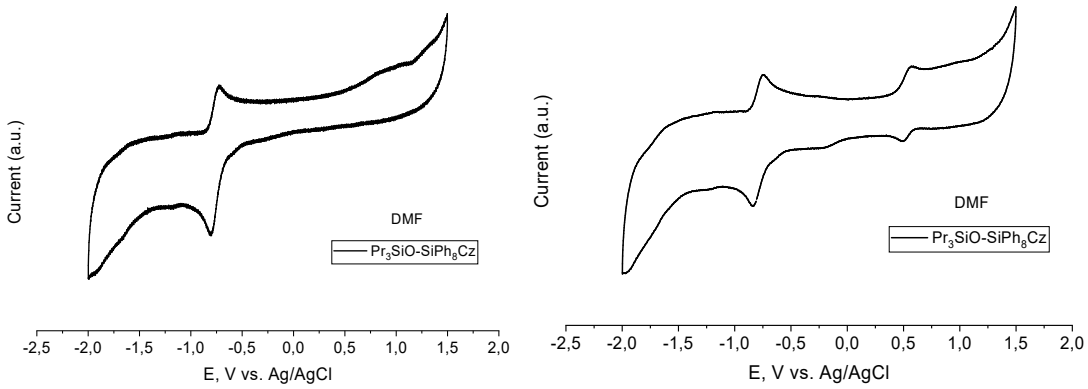

Figure S10,C. Cyclic voltamograms of $(Pr_3SiO)SiCzPh_8$ **(5a)** in DMF (left) and in DMF with ferrocene (right). Sweep rate was 25 mV/s.